Mon. Not. R. Astron. Soc. **000**, 1–1 (2019) Printed 25 April 2019 (MN LaTeX style file v2.2)

Deep Learning Applied to Galaxy Evolution: Clump Detection in CANDELS Galaxies

Christoph T. Lee[1]*, Marc Huertas-Company[2], Yicheng Guo[3], Joel R. Primack[1]
[1] *Physics Department, University of California, Santa Cruz, CA 95064, USA*
[2] *GEPI, Observatoire de Paris, CNRS, Université Paris Diderot, 61, Avenue de l'Observatoire, F-75014 Paris, France*
[3] *Department of Physics and Astronomy, University of Missouri, Columbia, MO 65211, USA*

Accepted XXX. Received YYY; in original form ZZZ

ABSTRACT
Abstract here.

Key words: Keywords

1 INTRODUCTION

The analysis has two main parts that can be broken into sections or subsections: (1) model architecture, training set composition, model performance on test set, and (2) CANDELS sample, clump detection statistics in CANDELS and comparison to Guo clump detection, clump detection in Guo "simulated" CANDELS images and comparison to Guo detection, clumpy galaxy fraction and comparison to Guo, and extension of these statistics / results into additional wavebands (b,v,i) for all galaxies in range z = 0.5-3. Are there any important sections missing from this list, or ones that should be skipped over?

2 MODEL DESIGN AND METHOD

2.1 Model Architecture

2.2 Training Set

2.3 Performance

3 CLUMPS IN CANDELS

3.1 Galaxy Sample

3.2 Comparison of Results

3.2.1 Purity and Completeness

3.2.2 Clump Detection Probability

3.2.3 Fraction of Clumpy Galaxies

3.3 Multi-band Clump Detection

4 DISCUSSION

5 CONCLUSIONS

ACKNOWLEDGEMENTS

We acknowledge stimulating discussions with ...

REFERENCES

This paper has been typeset from a TeX/ LaTeX file prepared by the author.

* E-mail: chtlee@ucsc.edu

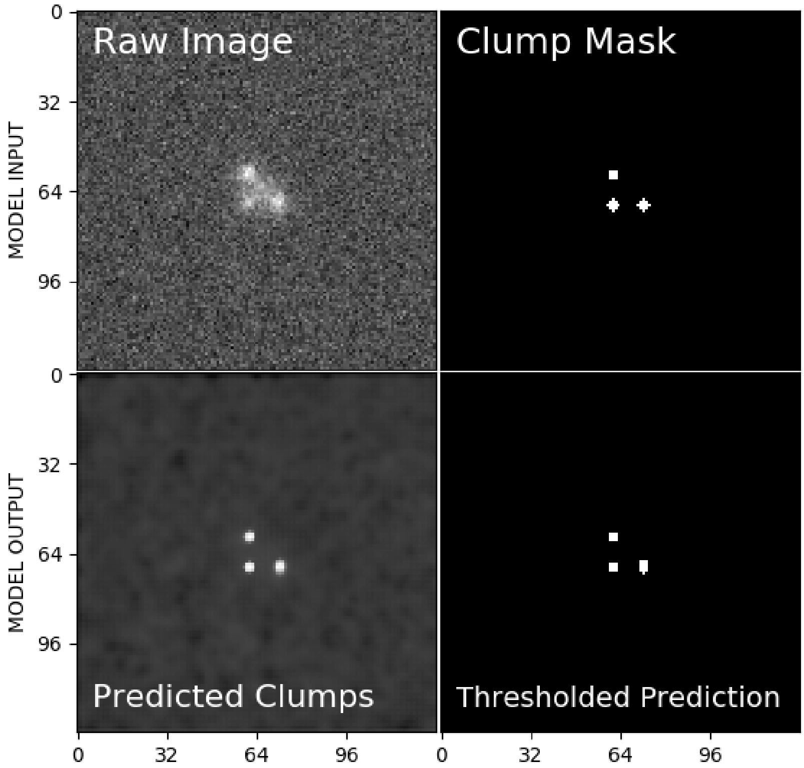

Figure 1. Example of model performance on GalSum test image. The top left and right panels show the raw GalSim test image and true clump mask, respectively. The bottom left and right panels show the model output (predicted clumps) and thresholded model output, respectively. This example galaxy contains three true clumps clump mask, all of which are identified with high confidence and precision by the model. We use a threshold value for the lower right panel determined by For the lower right panel we use the threshold value that optimally reduces error between the thresholded model output and true clump mask across the entire test set.

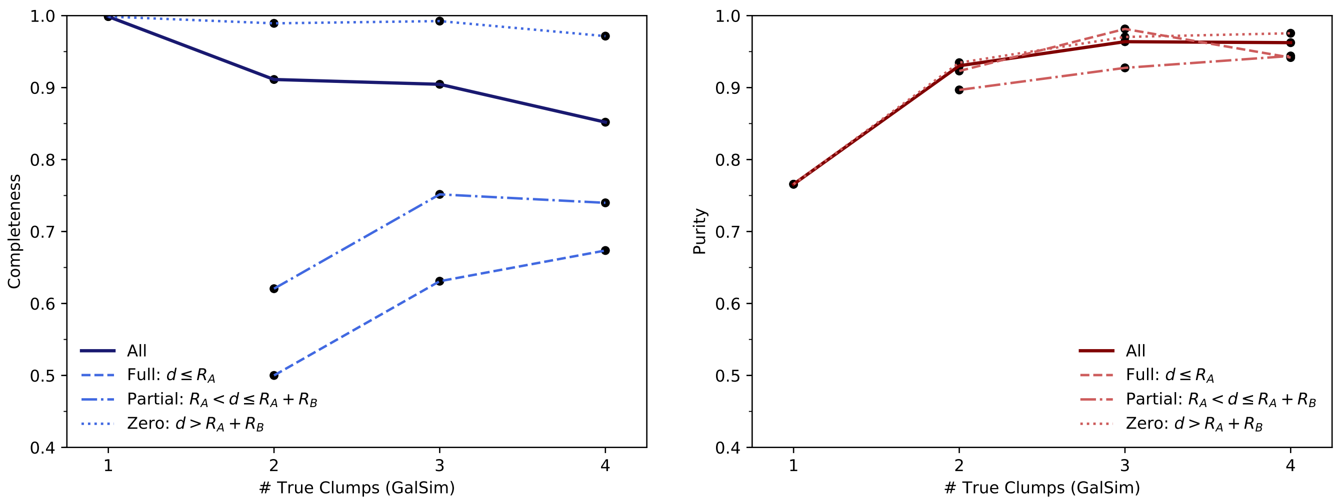

(a) Completeness

(b) Purity

Figure 2. Completeness and Purity of predicted clump catalog compared to the true clump catalog for the v-band optimized GalSim test set as a function of the number of true clumps per galaxy. Completeness describes the fraction of true clumps the model also finds, while Purity represents the fraction of predicted clumps that are also true clumps. We see that overlapping true clumps (i.e. cases where an individual GalSim image has two or more overlapping clumps) are much more difficult for the model to correctly recover. In this case, R_A refers to the radius of the larger clump (if they are different sizes), and R_B is the radius of the smaller clump. Clumps that overlap partially, but still have distinct centers, are segregated from those that fully overlap (i.e. both centers are within the larger clump). For non-overlapping clumps ($d > R_A + R_B$), we see that the model achieves nearly perfect completeness and better than 90% purity in most cases. The drop in purity for galaxies with only one clump probably reflects the model's tendency to identify the galaxy center as a clump as well in some cases of low luminosity, high relative clump flux, single-clump galaxies.

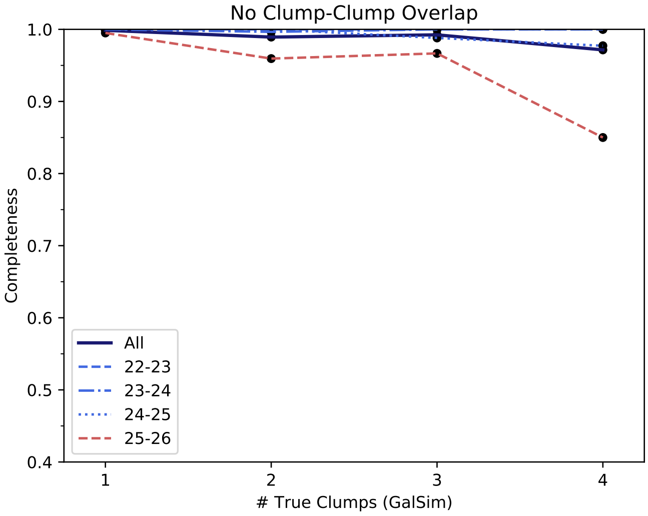

(a) Completeness

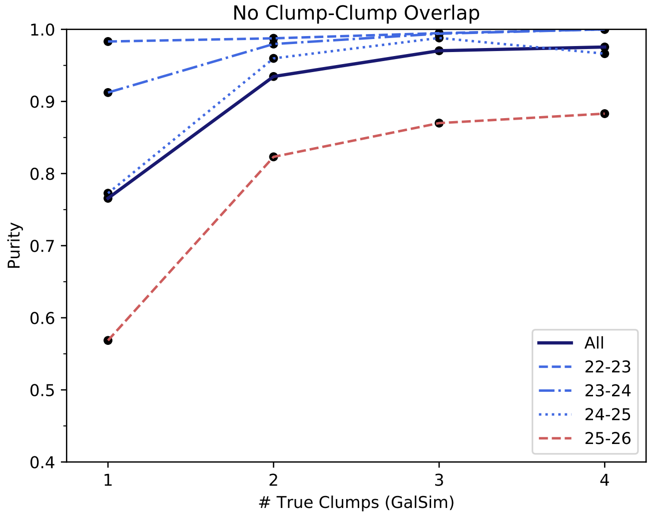

(b) Purity

Figure 3. Completeness and Purity of predicted clump catalog compared to the true clump catalog for the v-band optimized GalSim test set as a function of the number of true clumps per galaxy, binned by galaxy AB magnitude. Completeness describes the fraction of true clumps the model also finds, while Purity represents the fraction of predicted clumps that are also true clumps. We show results for non-overlapping clumps only. The Model achieves nearly perfect completeness for all but the faintest galaxies. Purity remains better than 90% for galaxies with multiple clumps except for the faintest magnitude bin.

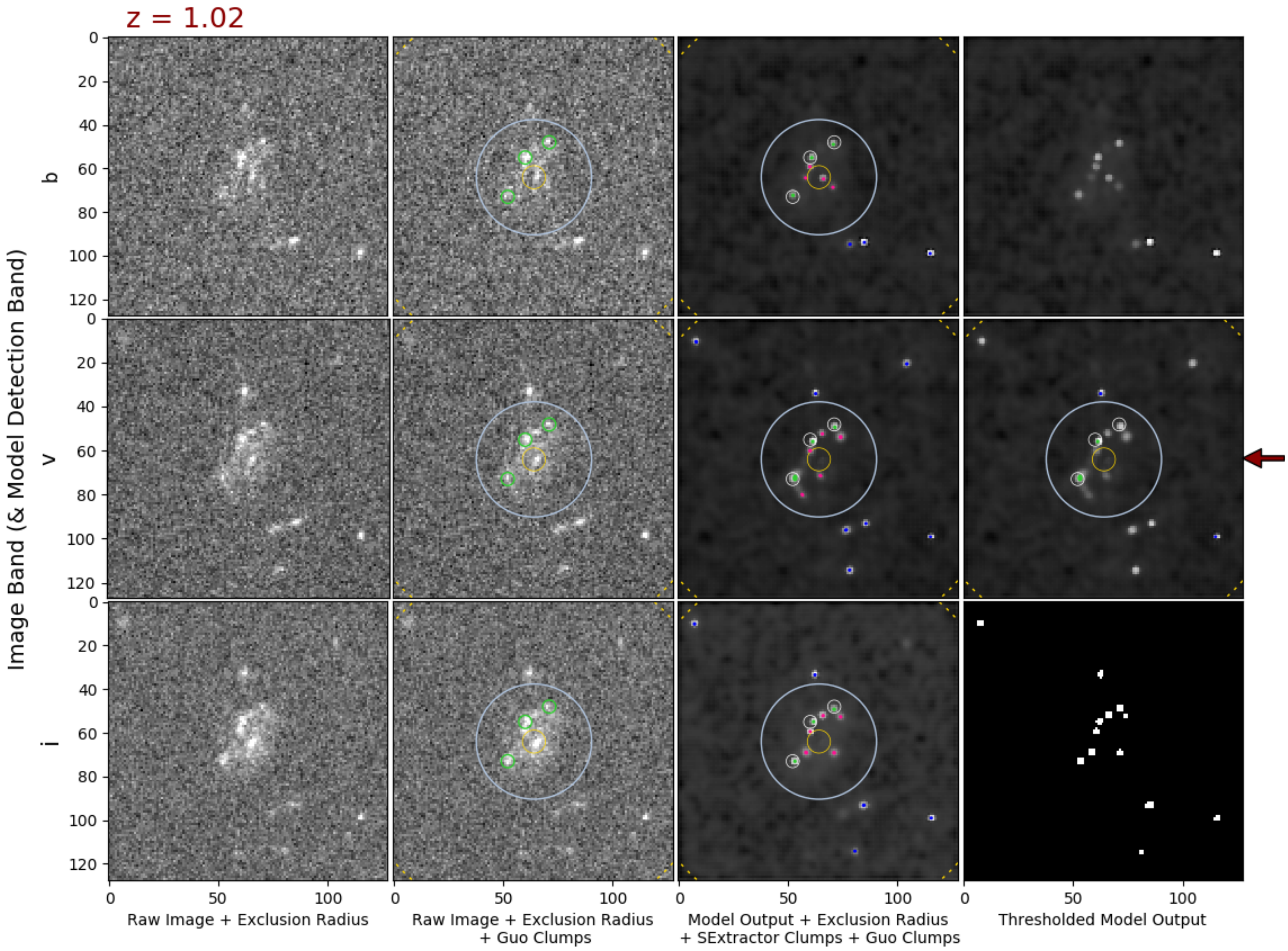

Figure 4. We show for an example CANDELS galaxy how our new deep learning based clump finder compares to the clumps identified in the Guo15 analysis. The top row of panels are based on the b-band galaxy image, the middle row shows the results in v-band, and the bottom row show the results in i-band. The panels in the leftmost column are the unmodified 128x128 pixel cutouts of the galaxy. In the second column from the left, we overlay several circles onto the raw galaxy image. The small thin yellow circle in the center of each panel encloses $0.5R_e$, the thin blue circle encloses $2.5R_e$, and the large dotted yellow circle (only visible in the corners of each panel) encloses $8R_e$, where R_e is the half light radius of the galaxy. The green circles represent clumps that Guo15 identified for this galaxy. Note that Guo15 identified clumps only in the rest-frame UV band, which for the redshift range $1 \leqslant z < 2$ is v-band (also denoted by the bold red arrow on the right side of the plot). Consequently, we highlight the Guo15 clump locations in each band, but only compare directly to our new clump finder in the v-band image for this galaxy. In the third column from the left, we show our deep learning model output image, given the raw galaxy image (left most panel) as input. We have overlaid this output image with the same concentric radii markers as described for the second column, except that now any Guo15 clumps are shown in light gray circles. Additionally, we color each of the segmentation regions that SExtractor identifies as a source in the model output. SExtractor sources that align with the Guo15 clumps are colored green, those that lie outside of the $2.5R_e$ exclusion radius are colored blue (ignored), and any remaining sources are colored pink. The final (4th) column shows a mixed representation of the model output. The top panel shows the raw model output with no overlaid information, the panel from the middle row shows the same information as the panel in the 3rd column from the middle row, but now only coloring those sources that pass the Guo15 purity-boosting criteria (i.e., ignoring clumps that are low confidence, low brightness, or very close to the center). The bottom panel on the last column shows the thresholded model output for the i-band prediction, to provide an example output binary clump mask. For this galaxy, we find that our deep learning model finds the same v-band clumps that Guo15 did, but also finds several additional low brightness clumps. Note that because we did not classify the galaxy bulge as a clump when training our model, the model often does not identify bright central objects as clumps, as is the case in particular in the i-band image of this example. Visual inspection of the raw galaxy image, model output, and predicted clumps seems to corroborate the success of the deep learning based clump finder for this example galaxy.

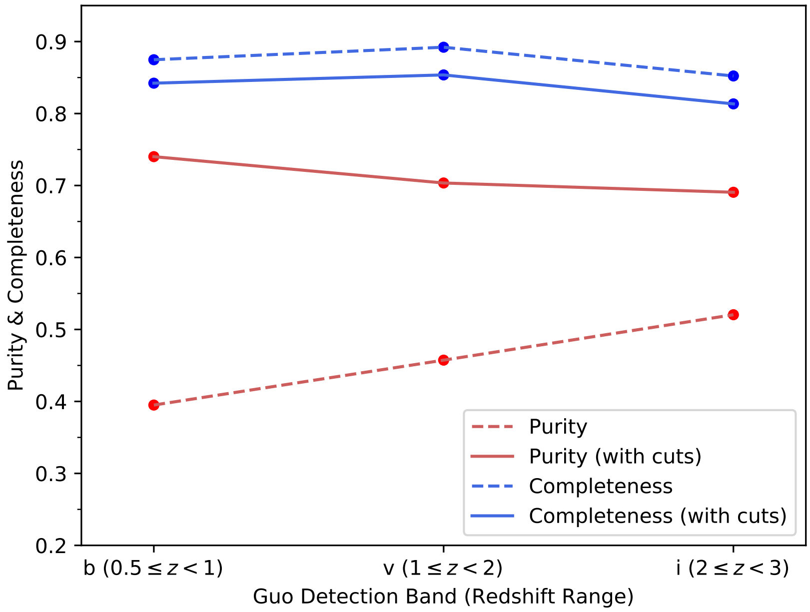

Figure 5. Example of model performance on test image.

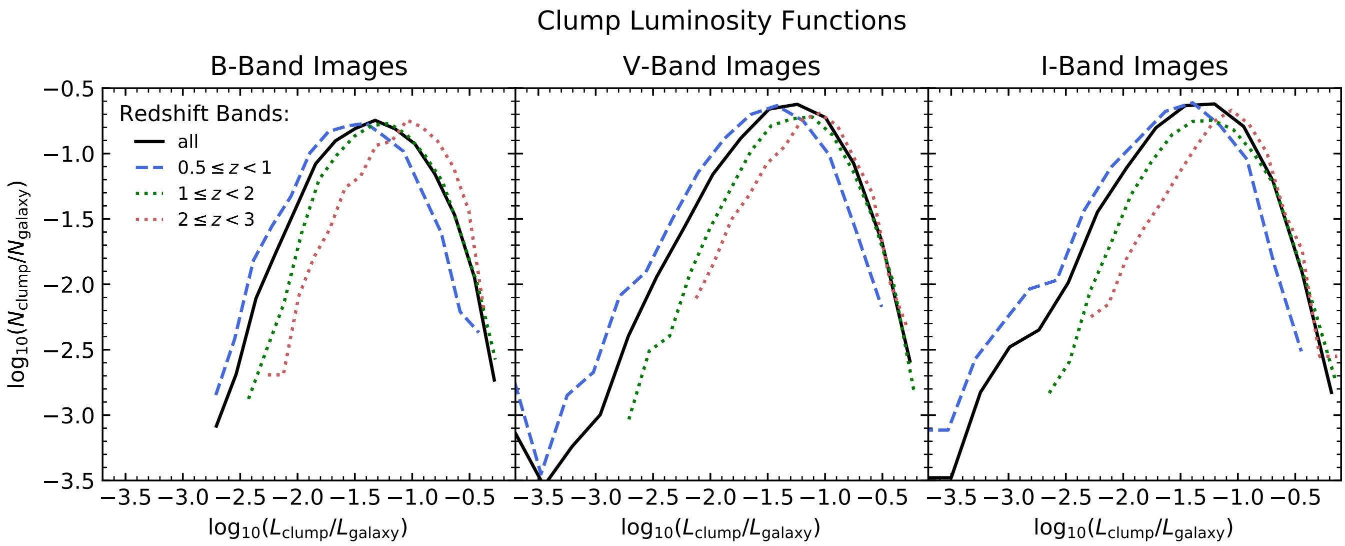

Figure 6. Example of model performance on test image.

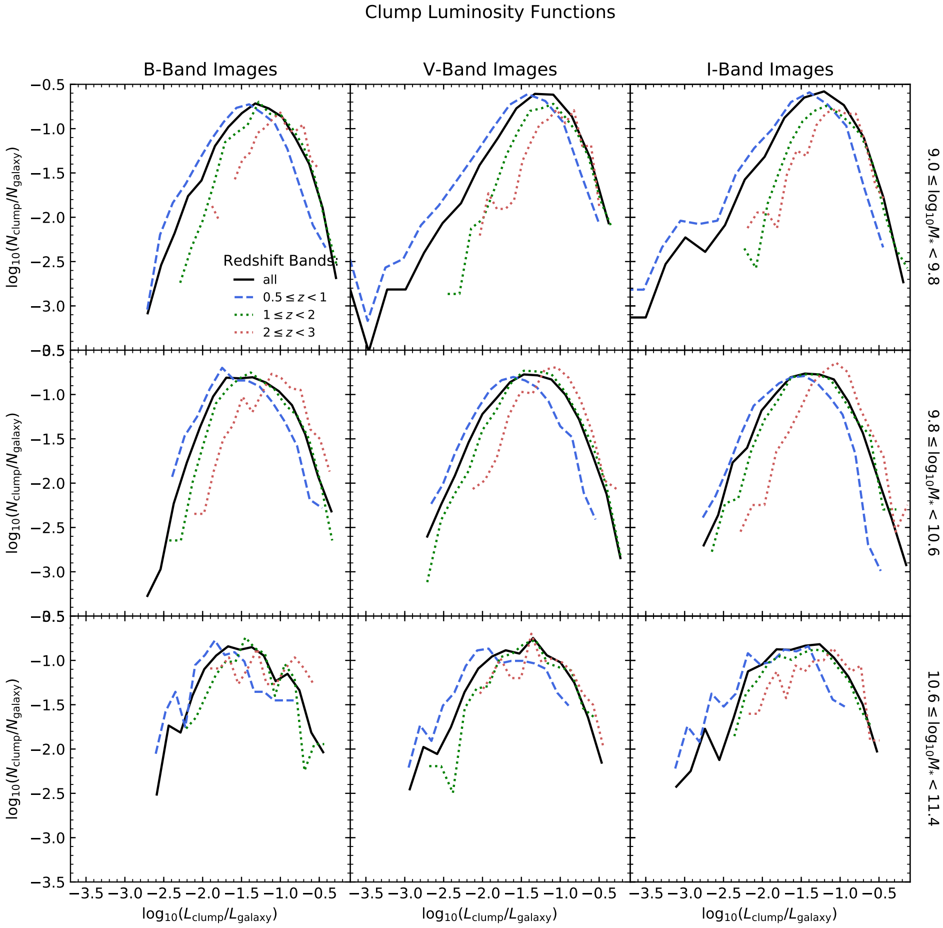

Figure 7. Example of model performance on test image.

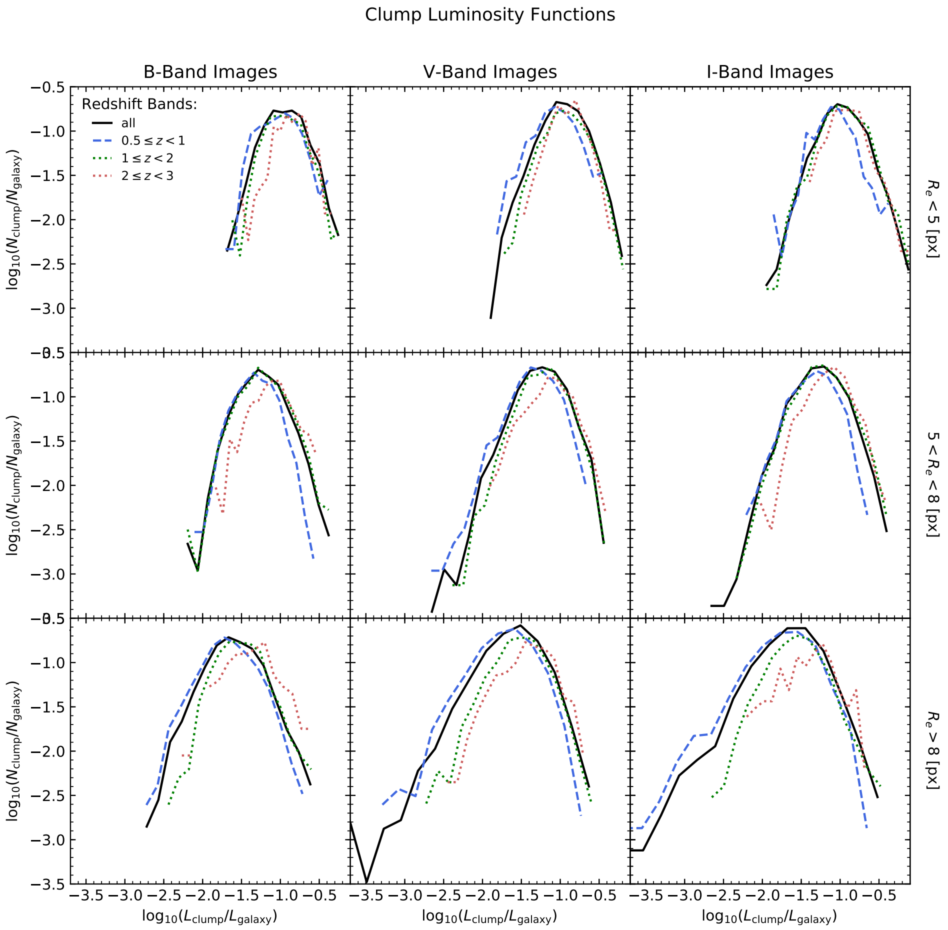

Figure 8. Example of model performance on test image.

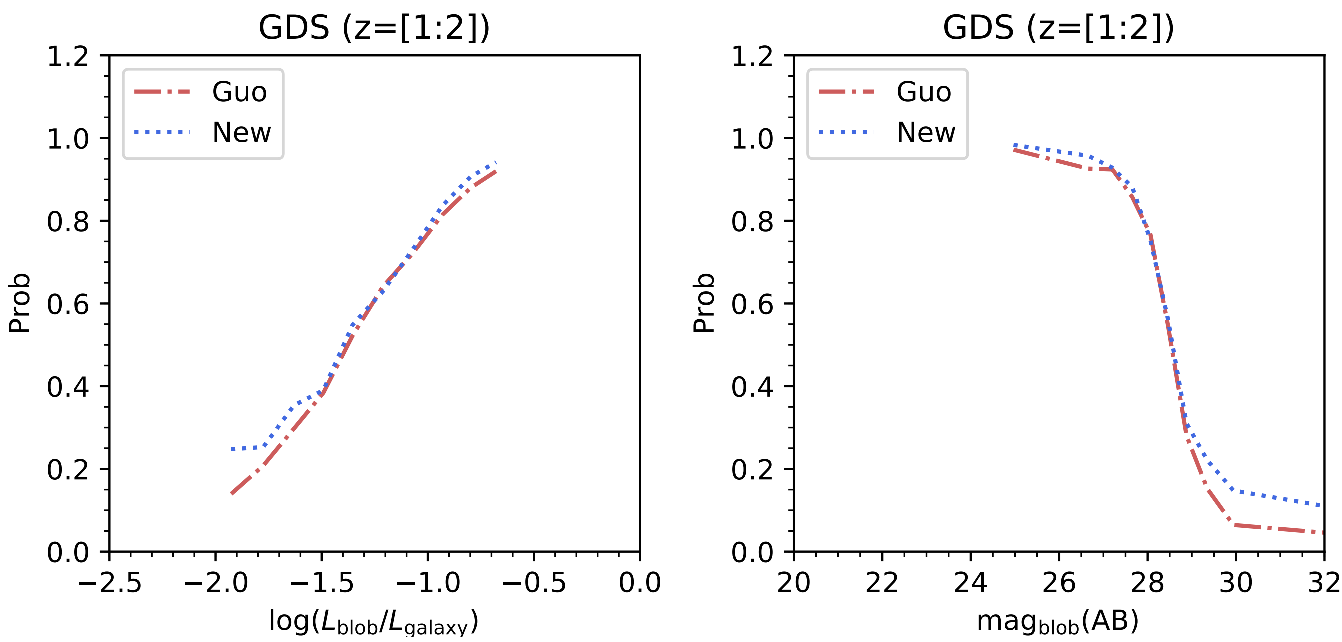

Figure 9. Example of model performance on test image.

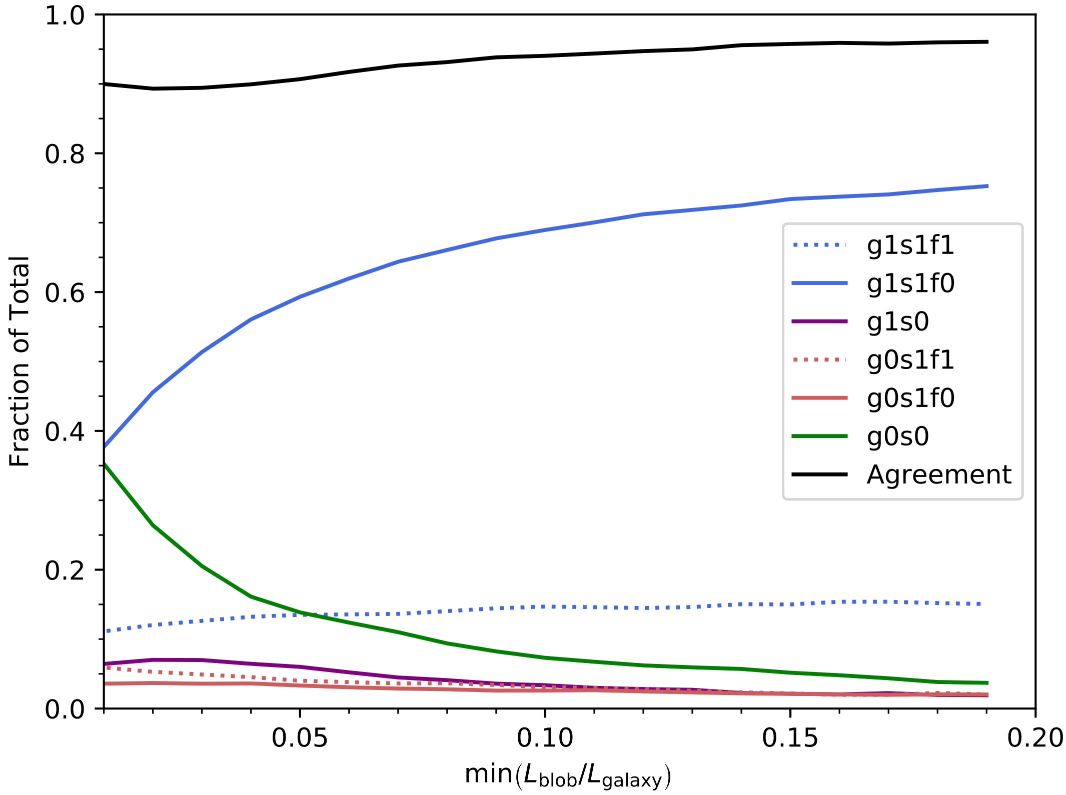

Figure 10. Example of model performance on test image.

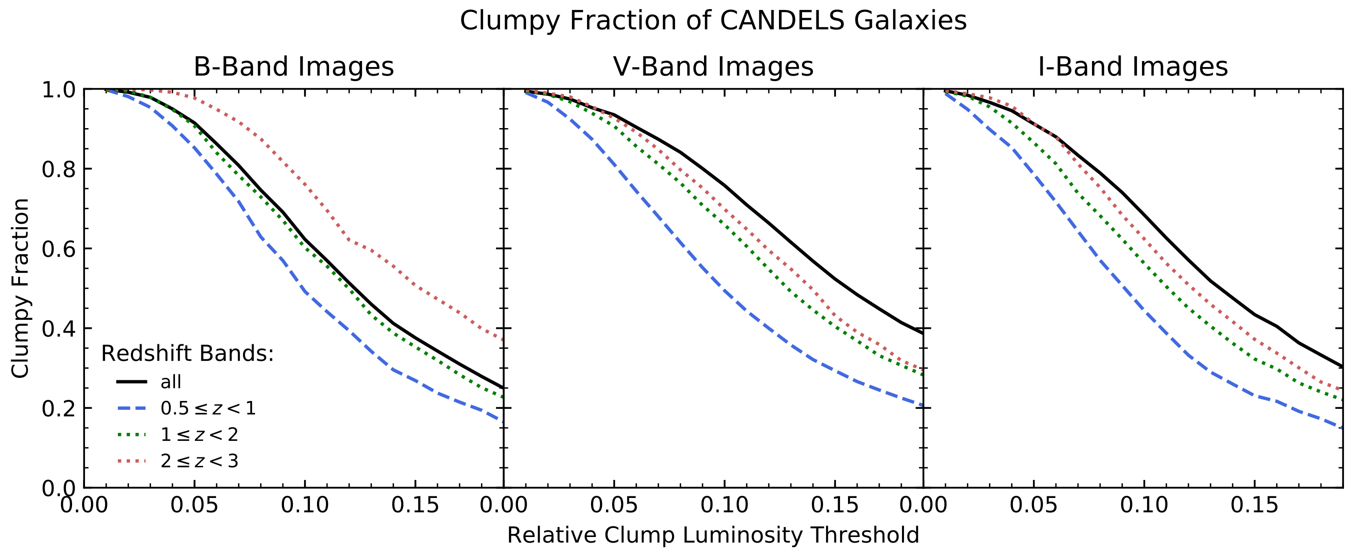

Figure 11. Example of model performance on test image.

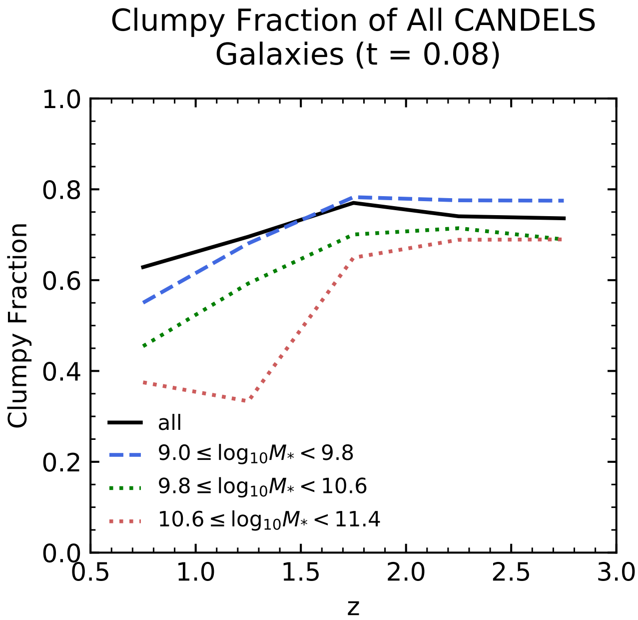

(a) label 1

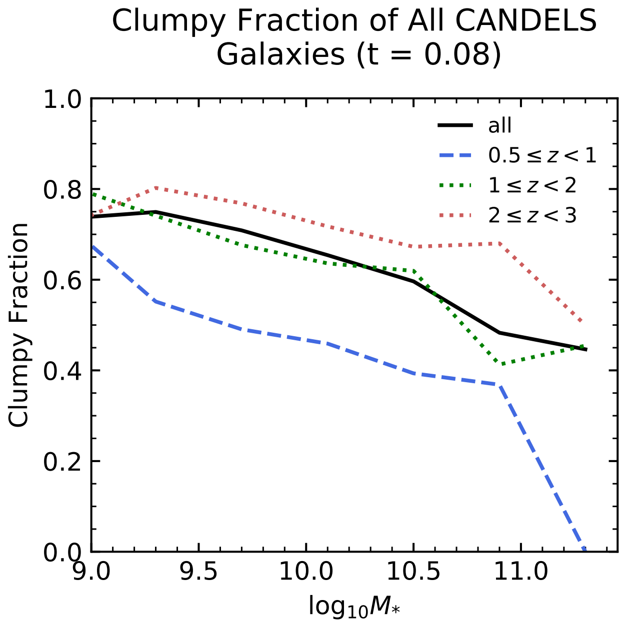

(b) label 2

Figure 12. 2 Figures side by side

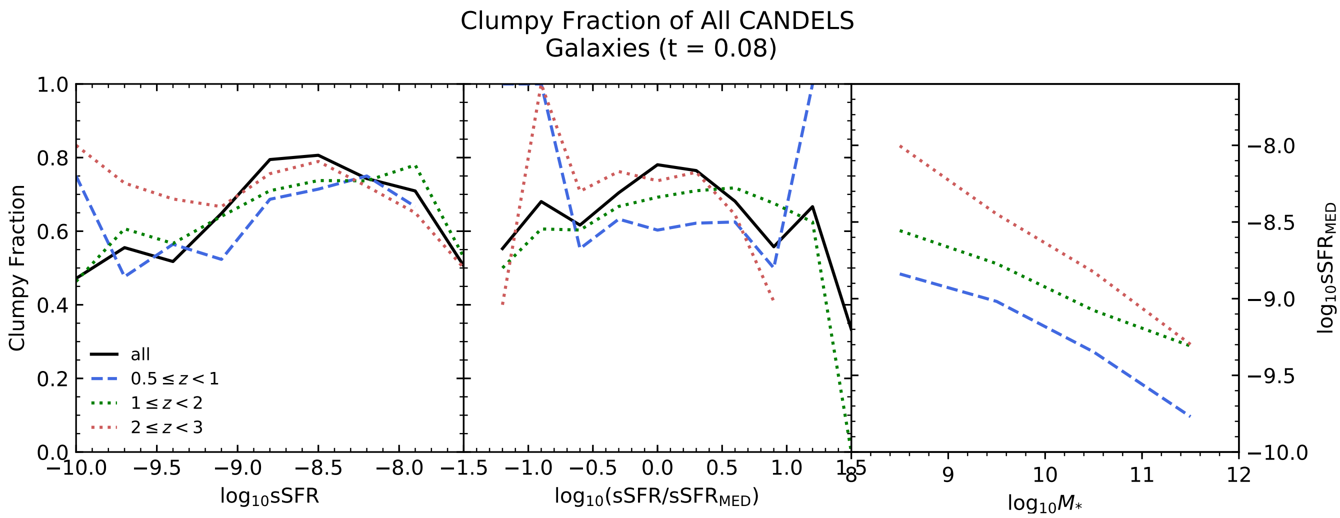

Figure 13. Example of model performance on test image.

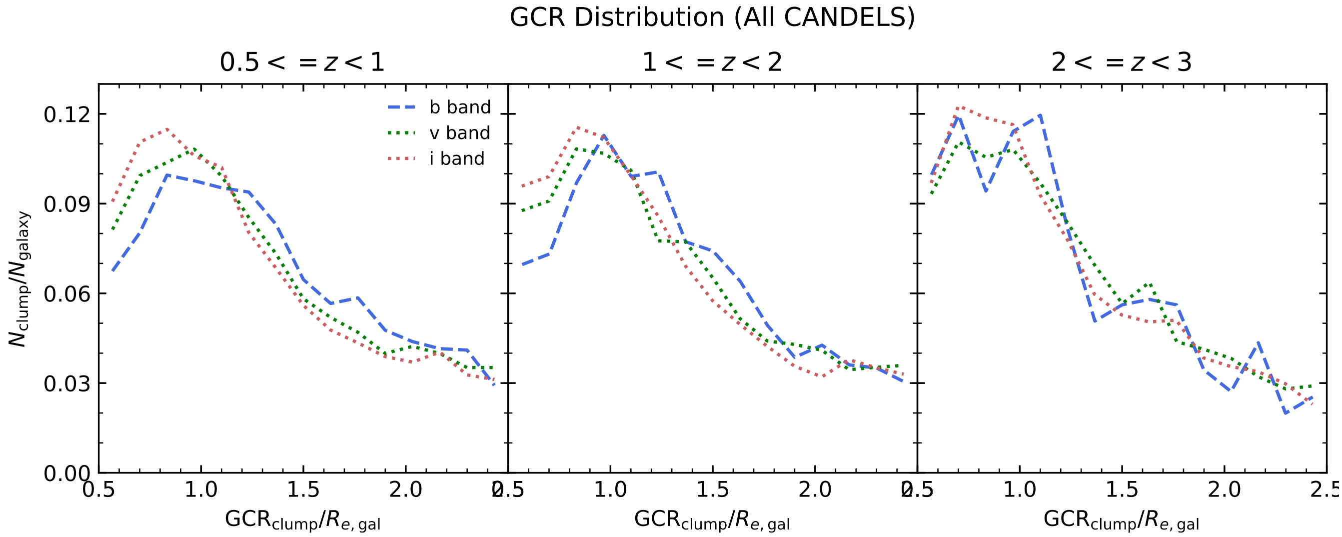

Figure 14. Example of model performance on test image.